

# A First Close Look at the Balmer Edge Behavior of the Quasar Big Blue Bump

Makoto Kishimoto<sup>1\*</sup>, Robert Antonucci<sup>2</sup> and Omer Blaes<sup>2</sup>

<sup>1</sup>*Institute for Astronomy, University of Edinburgh, Blackford Hill, Edinburgh EH9 3HJ, UK*

<sup>2</sup>*Physics Department, University of California, Santa Barbara, CA 93106, USA*

20 March 2019

## ABSTRACT

We have found for the first time a Balmer edge feature in the polarized flux spectrum of a quasar. The edge feature is seen as a discontinuity in the slope, rather than as a discontinuity in the absolute flux. Since the polarized flux contains essentially no broad emission lines, it is considered to arise interior to the broad emission line region, showing the spectrum with all the emissions outside the nucleus scraped off and removed. Therefore, the polarized flux spectrum is likely to reveal features intrinsic to the Big Blue Bump emission. In this case, the existence of the Balmer edge feature, seen in absorption in the shorter wavelength side, indicates that the Big Blue Bump is indeed thermal and optically thick.

**Key words:** quasars - galaxies: active - accretion - polarization - radiation mechanisms: general

## 1 INTRODUCTION

Studies of the spectral energy distribution of quasars have shown that, among the various apparent components present, the most energetically dominant component is in the optical/UV (e.g. Sanders et al. 1989). However, rather surprisingly, the emission mechanism of this component, often called the Big Blue Bump (BBB), has not been well understood. Although the BBB is often assumed to be from optically-thick thermal emission from an accretion disk, observations are hardly said to be well described by simple disk models (Antonucci 1988, 1999; Koratkar & Blaes 1999). The current situation is that various disk models are still trying to accommodate the main features observed.

Among several serious problems are the continuum slope and apparent lack of continuum edges. In order to explain the observed optical/near-UV slope (e.g.  $F_\nu \propto \nu^{-0.3}$ , Francis et al. 1991; Neugebauer et al. 1987), the overall disk temperature has to be rather low (Koratkar & Blaes 1999). However, naively, at least in such a cool disk, its atmosphere would show large continuum edges. Apparently, we do not observe such features at the Lyman edge (Antonucci, Kinney & Ford 1989; Koratkar, Kinney & Bohlin 1992). This could possibly be accommodated by sophisticated disc atmosphere models (e.g. Hubeny et al. 2000), where the spectrum integrated over radii are smeared through the relativistic Doppler shifts

and gravitational redshifts. In these models, the flux discontinuity at the Lyman limit is rather well smeared. There is instead a slope change near the Lyman limit which is accompanied by an emission bump just longward of the change (Hubeny et al. 2000). Some quasar composite spectra (e.g. Zheng et al. 1997), as well as some individual spectra (e.g. 3C273, Kriss et al. 1999), show a slope change near this wavelength. But the predicted emission bump is not seen and it appears at the moment that the model slope change is not in a satisfactory agreement with the observed ones (Blaes et al. 2001).

Another problem is the magnitude and direction of polarization. A simple disk atmosphere would show the polarization equal to the classical case of the plane parallel electron scattering atmosphere which has  $P$  of 0 – 11.7% for the inclination angle of 0 – 90°, with the direction of polarization (direction of Electric vector vibration) perpendicular to the disc symmetry axis (Chandrasekhar 1960). The observed polarization of the BBB emission is typically  $\sim 1\%$ , and the position angle of polarization is *parallel* to the radio jet structure, when observations are available, which is presumed to be parallel to the disc axis. More recent calculations show that absorption opacity and general relativistic effects (Laor, Netzer & Piran 1990) and Faraday depolarization with magnetic fields in the disc atmosphere (Agol & Blaes 1996; Agol, Blaes & Ionescu-Zanetti 1998) can reduce the magnitude of polarization. The inconsistency in the direction of polarization will still remain, but absorption opacity effects might in some cases

\* E-mail: mk@roe.ac.uk

**Table 1.** Observation log at Keck I

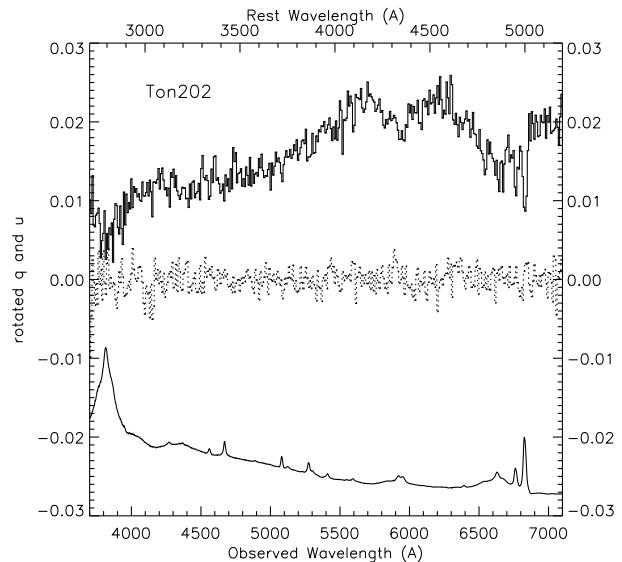
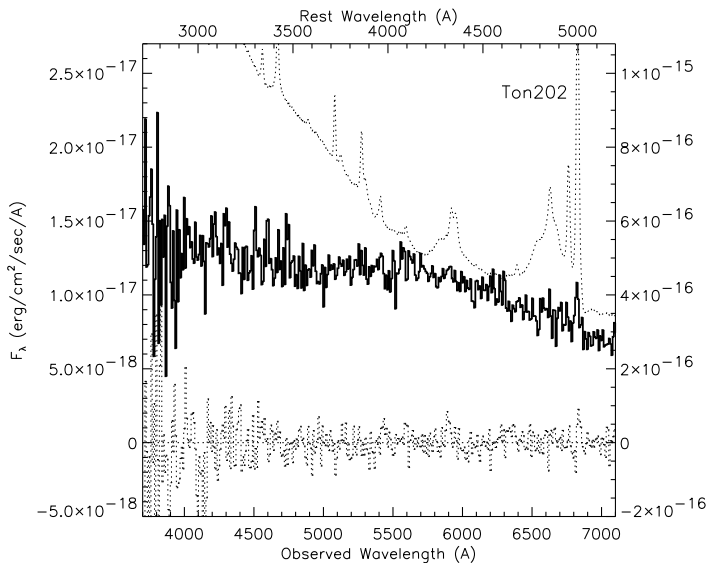
Name	redshift	slit PA ( $^{\circ}$ )	Exposure time (min)
Ton 202	0.366	72	30 $\times$ 2
Ton 202		102	30 $\times$ 2
4C37.43	0.371	95	30 $\times$ 2

flip the polarization direction (first noted by D.I. Nagirner, as described by Gnedin & Silant'ev 1978), and a rough surface of the discs might lead to the parallel polarization (Coleman & Shields 1990). Alternatively, the disk radiation is completely depolarized and then re-polarized slightly in the parallel direction by surrounding gas.

While the Lyman edge feature could be smeared by the relativistic Doppler shifts and gravitational redshifts in the disk atmosphere models, these will be less effective at smearing the Balmer edge feature. This is simply from a robust prediction of the disk models that the Balmer edge region of the spectrum originates from farther out in radius than the Lyman edge region. This should all be true even though the accretion disc stellar atmosphere models of the Lyman and Balmer edge features are still plagued by considerable uncertainties (see e.g. Hubeny et al. 2000, Hubeny et al. 2001 for discussion). Comptonization may also smear the Lyman edge (Czerny & Zbyszewska 1991), but as this is more important in high temperature regions, the Balmer edge should be less affected (see e.g. Fig.8 of Hubeny et al. 2001). In addition, aside from the disk models, the Lyman edge feature, which is due to a resonant transition, could rather easily be imprinted by a foreground absorption, but this is less likely for the Balmer edge. The Balmer edge should therefore be a key target wavelength region. The observation of this wavelength range not only could test an accretion model, but more fundamentally, could extract direct evidence for the thermal nature of the BBB emission. Even this fundamental issue has not been shown directly, and this lack of direct evidence for the emission nature has been one of the main sources of the controversy.

The only problem with checking this empirically is that the Balmer edge wavelength region of the BBB emission is very hard to observe due to the Balmer emission lines/continuum and FeII emission lines from the Broad Line Region (BLR) and outer regions (called the 3000Å bump, or the small blue bump). However, we can sometimes remove all these unwanted emissions by taking a polarized flux spectrum. As mentioned above, many quasars are found to be polarized at  $P \sim 1 - 2\%$ , and at least in some cases, emission lines (broad and narrow) are unpolarized - the polarization is confined to the continuum (Schmidt & Smith 2000; Antonucci 1988, showing the data of Miller and Goodrich). This indicates that the polarization mechanism resides interior to the BLR in these cases. Thus, the polarized flux shows the spectrum interior to the BLR, revealing the underlying behavior at the Balmer edge region.

We have obtained high S/N spectropolarimetry data of quasars with the Keck telescope, which allow us to investigate this Balmer edge behavior in detail. We report in this paper that we have indeed found a Balmer absorption feature in one of the quasars we observed.

**Figure 1.** Rotated normalized Stokes parameters  $q$  and  $u$  for Ton 202 binned with 4 pixels ( $\sim 9\text{\AA}$ ). The bottom spectrum is the scaled Stokes  $I$  (total flux in  $F_{\lambda}$ ) for reference.**Figure 2.** Rotated, unnormalized Stokes parameters  $Q$ , corresponding to  $P \times F_{\lambda}$ , and  $U$  (flux scale is on the left axis) for Ton 202 binned with 4 pixels ( $\sim 9\text{\AA}$ ), along with the scaled Stokes  $I$  (flux scale is on the right axis).

## 2 OBSERVATION

We have observed two quasars listed in Table 1 on May 8, 2002 (UT) with LRIS on the Keck-I telescope using its polarimetry module. These quasars are (1) polarized but known to have no emission lines in the polarized flux spectrum of limited S/N in the literature (2) in the redshift range of  $z \sim 0.3$  to have the Balmer edge in the observed frame fall on the appropriate wavelength range for the instrument sensitivity and sufficiently far from the atmospheric cutoff. We have used LRIS blue-side CCD with grism 300/5000 giving a resolving power of about 300. The sampling was  $2.2\text{\AA}$  per pixel, and  $0.''215$  per pixel in the spatial direction. The

data were obtained with the slit approximately along the parallactic angle. The slit width was  $1.''5$ .

The data were reduced in the standard manner: the bias level was subtracted using the overscan region, frames were flat-fielded using dome flat exposures, and obvious cosmic-ray hits were removed and interpolated using neighboring pixels. Then the polarimetry data reduction was done following Miller et al. (1988). We lost the first hours of the night with clouds, and some of the subsequent observations might have been through cirrus, which may have caused a little guide error. We have checked the balance factor  $\omega$  spectra (Miller et al. 1988) and object positions for each pair of two frames taken with the waveplate rotated by  $45^\circ$ , and also checked the consistency of  $q$  and  $u$  between different pairs. We have excluded the pairs which had an obvious guide problem and/or whose  $\omega$  spectra had a strong curvature over the wavelengths. The sets in which the  $q$  or  $u$  is systematically different from other sets were found only in these excluded frames. From the 4 sets of 4 frames (4 waveplate positions) left for Ton 202 and 2 sets left for 4C37.43 (listed in Table 1), the normalized  $q$  and  $u$  were obtained. The Stokes  $I$  was obtained from the same two sets for 4C37.43, but for Ton 202, it was obtained from three sets, excluding one which showed a slight curvature in the  $\omega$  spectrum. The Stokes  $I$ 's were flux-calibrated using the standard star BD+33d2642.

Due to a problem at the end of the night, we lost the time for the polarization standard star observation. Therefore, there is an uncertainty of a constant in our measurement of the position angle (PA) of polarization. But this constant was roughly determined based on the published PAs of our targets, and the uncertainty is probably  $\sim 5^\circ$  from the probable variability of the PAs of the targets: the observed PAs in the literature are within  $\sim 5^\circ$  of  $70^\circ$  and  $105^\circ$  for Ton 202 and 4C37.43, respectively, except for one occasion in each target (Berriman et al. 1990, Schmidt & Smith 2000; see section 4.3).

The unpolarized standard star was also BD+33d2642. This star is reported to be slightly polarized with  $P \sim 0.2\%$  (Schmidt, Elston & Lupie 1992). We also find this level of polarization but at PA of  $\sim 100^\circ$  as opposed to  $\sim 10^\circ$  reported by Schmidt et al. (1992). We believe that the PA in Schmidt et al. is in error by  $90^\circ$  for the following reasons. (1) The overall tendency of interstellar polarization around the star is at around PA  $100^\circ$ . (2) We looked at another data set of the same star taken in Jan 1998 at Keck (given to us by A. Barth) and found the polarization consistent with ours. (3) Another Keck observation by Cimatti et al shows  $100^\circ$  (A. Cimatti, pc). Our  $P$  measurement shows a Serkowski-like curve, and matches well with Schmidt et al's multi-band  $P$  measurement, if rotated by  $90^\circ$ . Based on the difference between these data sets, the instrumental polarization is expected to be less than  $0.05 - 0.1\%$ . This is also supported by the comparison of two sets of our Ton202 observation which were taken in different slit directions (see also section 4.3).

At the red end of the spectrum  $\lambda \gtrsim 6600\text{\AA}$ , the spatial profile degrades (worse in the observation of 4C37.43, possibly due to larger flexure in the focus direction in LRIS from the lower attitude of the telescope). Therefore we have used rather large extraction windows to accommodate it,  $3.''7$  for Ton 202 and  $6.''7$  for 4C37.43, although there might still be

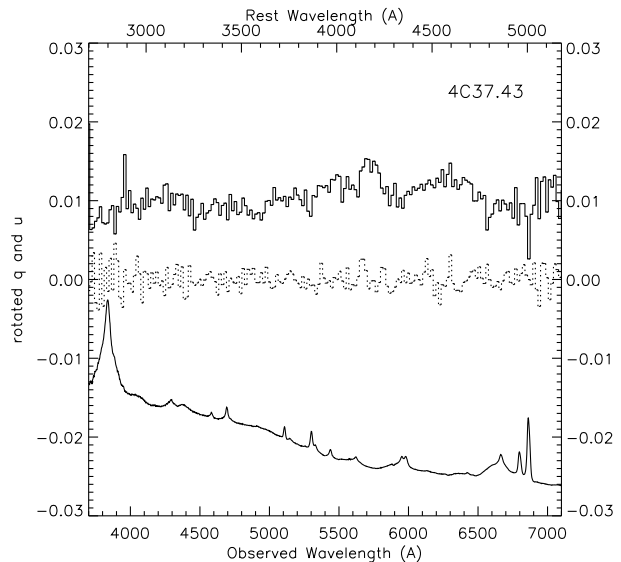


**Figure 3.** The same as Fig.1 but for 4C37.43 with 8 pixel bin ( $\sim 18\text{\AA}$ ).

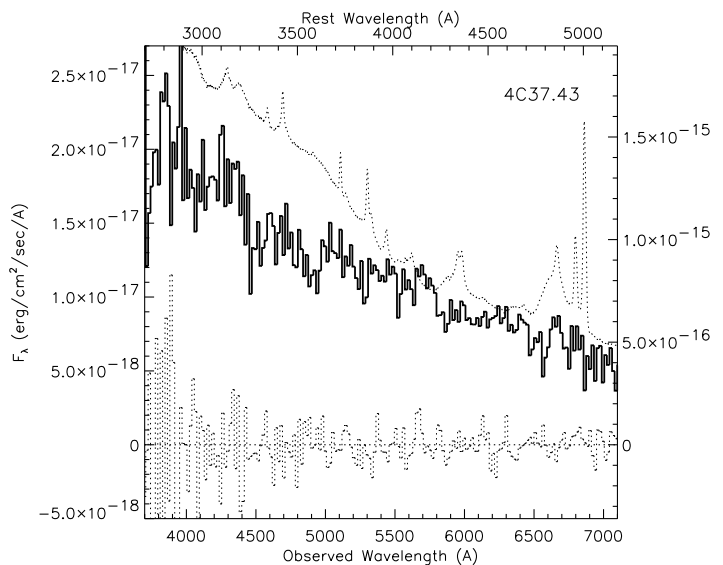


**Figure 4.** The same as Fig.2 but for 4C37.43 with 8 pixel bin ( $\sim 18\text{\AA}$ ).

a slight uncertainty in the  $P$  measurement at the reddest end.

### 3 RESULTS

#### 3.1 Ton 202

Figure 1 shows the normalized Stokes parameters  $q$  and  $u$  for the quasar Ton 202 at  $z = 0.366$ , along with the total flux  $F_\lambda$  at the bottom for reference. The reference axis of  $q$  and  $u$  has been rotated to be at the position angle (PA) of the object's polarization, which is essentially wavelength independent. Figure 2 shows unnormalized Stokes  $Q$  in thick lines, which is essentially the polarized flux spectrum  $P \times F_\lambda$ , and  $U$  in dotted lines at the bottom. The dotted spectrum

at the top is the total flux  $F_\lambda$  scaled to roughly match the polarized flux at the red side. The emission lines, both broad and narrow ones, are essentially all absent in the polarized flux to a high S/N, corresponding to the clear decrease of polarization at the emission line wavelengths (see Fig.1).

From Figure 2, the slope of the polarized flux at the red side is roughly the same as that of the total flux. However, we find that the slope of the polarized flux changes at the bluer side of  $\sim 4000\text{\AA}$  in the rest frame (note the rest wavelength scale at the top of Figures), just where the small blue bump starts in the total flux. There might also be a possible up-turn at the bluer side of  $\sim 3600\text{\AA}$  in the rest frame. To illustrate the slope change quantitatively, if we measure the slope at the blue side (2800 - 4000 $\text{\AA}$  in the rest frame) and the red side (4000 - 4900 $\text{\AA}$ ) by fitting a broken power law, we obtain  $\alpha = -1.73 \pm 0.07$  and  $-0.54 \pm 0.08$ , respectively, where  $F_\nu \propto \nu^\alpha$  (we have excluded the red end of the spectrum considering the possible uncertainty from the spatial profile degradation; see section 2).

We identify this to be a Balmer edge feature, seen in absorption in the shorter wavelength side. It certainly does not look like an “edge” seen in the continuum opacity. This is conceivable, since the real edge should consist both of the continuum edge and high order Balmer lines, so that the combined effect may well be that the edge feature starts rather at around 4000 $\text{\AA}$ , instead of 3646 $\text{\AA}$ . In addition, there may be absorption by metal lines, resembling the 4000 $\text{\AA}$  break in an old stellar population. Recall too that there may be a secondary dip/up-turn at  $\sim 3600\text{\AA}$  near where the actual edge is expected.

However, admittedly, the edge and absorption lines probably need to be broadened in order to be consistent with the observed spectral shape of the polarized flux. This could be attributed to a Doppler smearing due to a high velocity dispersion expected in the deep potential well at the nucleus (though in terms of accretion disc models, the smearing effect is smaller for the Balmer edge than for the Lyman edge, as discussed in section 1). Without referring to any particular model, however, the shape of the feature and the wavelength of the slope change strongly suggest that the feature is most likely to be a Balmer edge absorption feature.

### 3.2 4C37.43

The data for 4C37.43 ( $z = 0.371$ ) are shown in Figures 3 and 4 in the same manner as for Ton 202. The data are of lower S/N compared to those for Ton 202, but there might be a weak broad H $\beta$  emission line in the polarized flux in this object. This means that there might also be some contribution from the small blue bump in the polarized flux of this object, making our scraping method incomplete. Apparently, there does not seem to be a clear slope change in the polarized flux, but the plot in  $\nu F_\nu$  (Fig.8) might suggest a very slight slope change again around 4000 $\text{\AA}$ . This is still unclear in the slope measurements with a broken power law:  $\alpha = -0.17 \pm 0.11$  where  $F_\nu \propto \nu^\alpha$  in the blue side (2800-4000 $\text{\AA}$  in the rest frame) and  $\alpha = +0.06 \pm 0.23$  in the red side (4000-4700 $\text{\AA}$ , excluding the possible broad line component and the red-end portion).

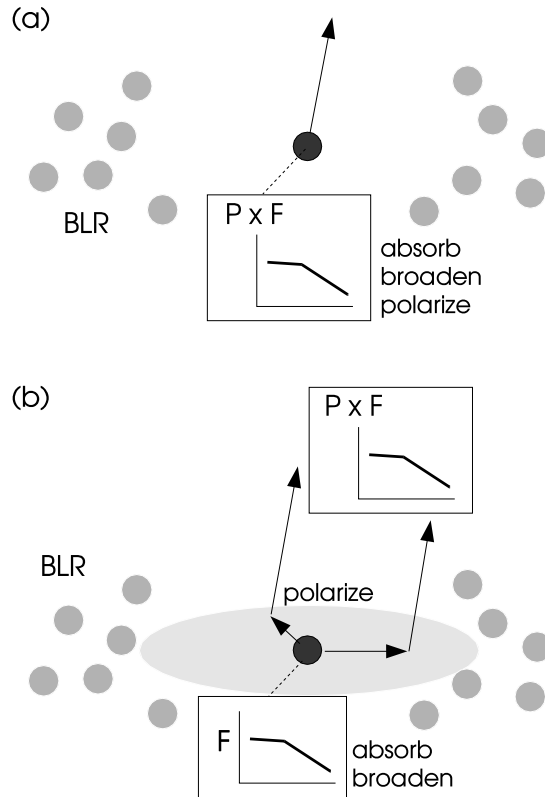


**Figure 5.** Schematic drawings of the possible geometric configurations. (a) The polarized flux is coming from the Big Blue Bump emitter at the centre. (b) The polarized flux is formed via scattering in the oblate electron scattering region surrounding the Big Blue Bump emitter.

## 4 DISCUSSION

### 4.1 The nature of the Big Blue Bump emission

As we have pointed out above, there are essentially no broad (and narrow) emission lines in the polarized flux of Ton 202, and the polarization is confined to the continuum. This means that the polarization seen here is very different from the polarization seen in many Seyfert 2 galaxies. In the latter, the continuum emission *and* the broad line emission are *both* scattered in the region exterior to the BLR and coming into our line of sight, so that both the continuum and broad lines are present in the polarized flux. In these Seyfert 2’s, the position angle of polarization is perpendicular to the radio jet structure. These two facts have led to the thought that the scattering region is located along the jet axis outside the nucleus and the BLR.

In contrast, in the case of Ton 202 where the broad lines are shown to be essentially unpolarized (and in other quasars shown in Schmidt and Smith 2000, though with a limited S/N), the region which is causing the polarization should be *interior* to the BLR (unless the polarized light is a completely different component from the BBB emission; see the discussion below). Unlike the cases of the Seyfert 2’s above, we still do not have a good understanding of the polarization mechanism in these quasars. One of the main difficulties in disc atmosphere calculations is that disk atmospheres gen-

erally produce polarization perpendicular to the disk axis, while the position angle of polarization is observed to be *parallel* to the jet axis (the difference between the optical polarization PA and the radio jet axis is  $15^\circ$  and  $9^\circ$  for Ton 202 and 4C37.43, respectively, from Schmidt & Smith 2000). However, the non-existence of exact models for the parallel polarization does not affect our conclusion that the polarizing region (the region causing the polarization) should be interior to the BLR (see more below for the discussion of the size).

Geometrically, we can first think of two cases. (1) The source of the BBB emission and the polarizing region are essentially the same — the Balmer-edge absorption, its broadening, and polarization are occurring within the BBB emitter (see Fig.5a). One such an example is a disk atmosphere (aside from the inconsistency in polarization direction). The Balmer edge feature in the polarized flux can mean either that the total flux of the BBB has an edge feature with a wavelength-independent polarization, or the total flux is rather featureless but the polarization is low at shortward of the edge. In either case, the edge feature in the polarized flux is simply intrinsic to the BBB emission in the sense that the feature is formed within the BBB emitter. (2) The polarizing region is located somewhere between the BBB emitter and the BLR. One conceivable case is an optically-thin oblate electron scattering region surrounding an unpolarized BBB emitter (see Fig.5b). The region would be optically thin (see discussion below), oblate and perpendicular to the jet axis in order to produce the polarization parallel to the axis (see Brown & McLean 1977 for polarization calculation). We would not consider dust scattering since the region is essentially within the dust sublimation radius. The intrinsic BBB polarization might have been completely wiped out by Faraday depolarization. In this optically-thin scattering case, the polarized flux spectrum is simply proportional to the incident BBB emission, so that the edge feature should have been formed, again, within the BBB emitter.

Therefore, in both cases above, the Balmer-edge absorption feature identified in the polarized flux is intrinsic to the BBB emission. Thus the feature indicates that the BBB emission is indeed thermal. The fact that the edge feature is seen in absorption in the shorter wavelength side indicates that the emission is optically thick. This is our first, primary conclusion.

The possible weak broad line component in the polarized flux of 4C37.43 might suggest that the size of the polarizing region in this object is not much smaller than the size of the BLR, which might be the case *in general*. In this sense, the case (2) above may be preferred rather than case (1). The radius of the oblate electron scattering region might be extended as large as the inner radius of the BLR.

Many Seyfert 1 galaxies also show a few % level polarization in continuum (e.g. Goodrich & Miller 1994; Smith et al. 2002). When the radio structure is available, the radio axis is parallel to the optical polarization direction in the majority of the cases (Antonucci 1983, 2002; Smith et al. 2002). In contrast to our two quasars, broad lines are very clearly polarized in these Seyfert 1 galaxies. However, the broad line polarization integrated over the line profile is generally at a different PA than the continuum, and the PAs often show some systematic rotation within the line wavelengths (Goodrich & Miller 1994; Smith et al. 2002). This

might suggest that the polarizing region in these Seyfert 1s is not much larger than the BLR, and it may be closely related to the oblate scattering region discussed above.

## 4.2 Other possibilities

The two cases above are probably the simplest cases for producing the observed polarization. However, we cannot rule out some cases where the Balmer edge feature seen in the polarized flux is still not intrinsic to the BBB emission. There might be a case where the scattering medium in case (2) above is also imprinting the absorption feature on the polarized flux spectrum (while the incident BBB spectrum is featureless; see Fig.6a). In this case, however, we need to have an absorption optical thickness of order unity in the Balmer continuum along the size of this region. The broadening of the absorption feature also need to occur in this scattering/absorbing medium. This would require a rather large velocity dispersion, having to put this region, for example, in a rather deep potential well. Having too a significant absorption optical thickness, especially in a deep potential well, is rather equivalent to having the whole scattering region as the BBB emitter itself, so that the distinction becomes largely semantic. This region might also produce a significant soft X-ray absorption. The broadening might be due to the scattering by hot electrons, but in this case, a significant alteration of the X-ray Fe K $\alpha$  line might be expected (but see Czerny & Zbyszewska 1991).

Alternatively, the Balmer absorption feature could be imprinted in the featureless polarized flux by some foreground region (Fig.6b). The background source of a featureless polarized flux could be the BBB emitter itself or a completely different source (in this case, a high polarization is required for this secondary source), assuming that the polarized flux is somehow produced by e.g. synchrotron process or electron scattering within that source. This case would require some particular velocity structure in this foreground medium along the line of sight, to produce the apparent slope change. Also the absorption feature would be more significant in the Lyman edge region in this case, since the Lyman transition is a resonant one. Such Lyman edge absorption is not seen in quasars, though the UV data for Ton 202 itself are quite noisy (Lanzetta et al. 1993; the UV spectrum of 4C37.43 looks featureless at the Lyman edge). Note that, conversely, the slope changes at the Lyman edge region seen in some cases, as discussed in section 1, could be a foreground absorption, but this is less likely to be the case for the (non-resonant) Balmer edge region.

## 4.3 Variability

Our polarization measurement of 4C37.43 looks rather consistent with that of Schmidt & Smith (2000) in the red part of the spectrum. But in the bluer part, the  $P$  in our measurement is slightly higher by  $\sim 0.1 - 0.2\%$ , and the total flux looks also slightly bluer, leading to a bluer polarized flux color ( $\alpha = -0.11 \pm 0.07$  for  $\lambda_{\text{rest}} = 2800 - 4700\text{\AA}$  in our data, whereas  $\alpha = -0.8 \pm 0.2$  in Schmidt & Smith 2000). Compared with the data for Ton 202 in Schmidt & Smith (2000) and Antonucci (1988; data of Miller and Goodrich), the measured polarization in our data is slightly higher especially at

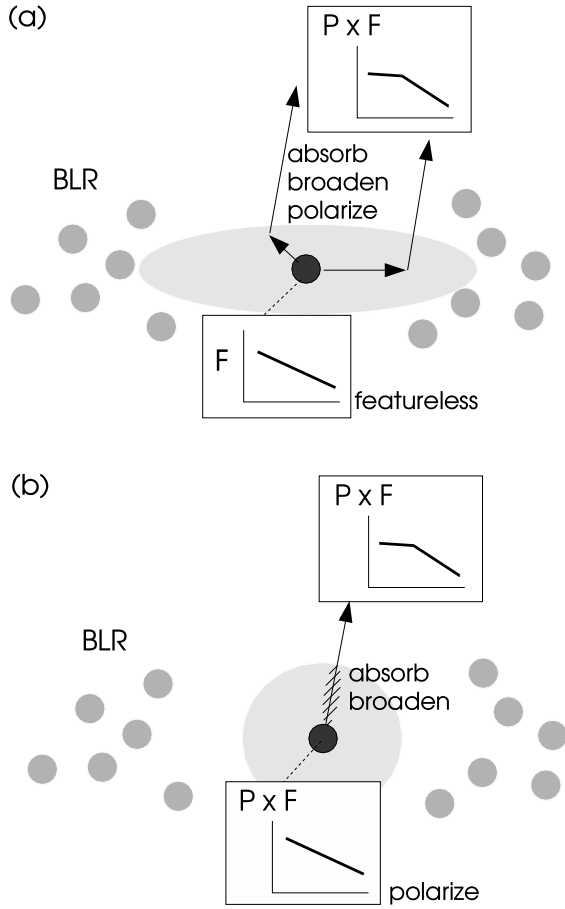


**Figure 6.** Schematic drawings for other possibilities. (a) The Balmer-edge absorption feature is formed within the scattering/absorbing region surrounding the Big Blue Bump emitter. (b) A broadened Balmer-edge feature is imprinted in a foreground region on an incident featureless polarized flux.

4000-4800Å in the rest frame of the quasar. The difference in  $P$  is up to 0.5%, which is much larger than the instrumental polarization level discussed in section 2. In the unlikely case that the identified edge-like feature in the polarized flux is solely due to the instrumental polarization, the  $q$  and  $u$  spectrum in the sky coordinates should look different in the data taken at different instrument angles (see Table 1), if the instrumental polarization stays the same in the instrumental coordinates. Since the instrument angles are different by 30°, the instrumental polarization component should rotate by 60° in the  $q$ - $u$  plane of the sky coordinates, which should obviously show up in the  $u$  spectrum. This is not the case, and the polarized flux spectra from two different instrument angles show essentially the same feature.

Therefore, the polarization of Ton 202, and probably also 4C37.43, seems to have varied slightly over these several years (from 1996-1999 to 2002). This is actually conceivable, since the polarization arises from a region smaller than (or in general, at most comparable to) the BLR, as we argued above. As noted in section 2, the polarimetric data of Berriman et al. (1990) and Schmidt & Smith (2000) which span from 1978 to 1999 have some evidence of variability for both of the objects (see section 4.2 of Schmidt & Smith

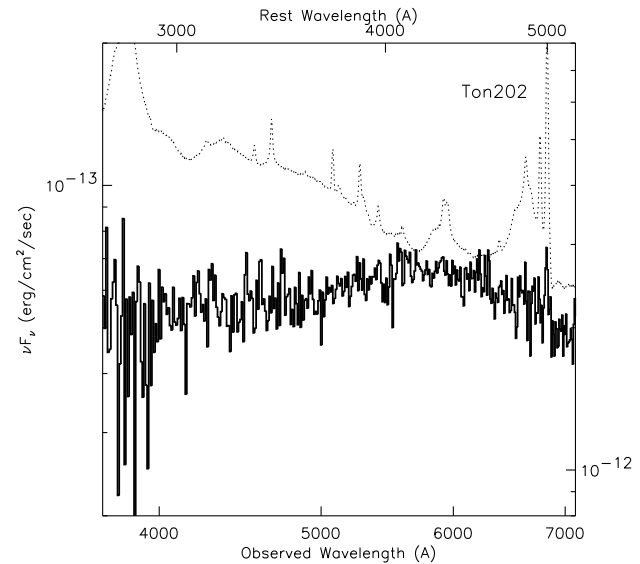


**Figure 7.**  $\nu F_\nu$  plot in log scale for Ton 202.

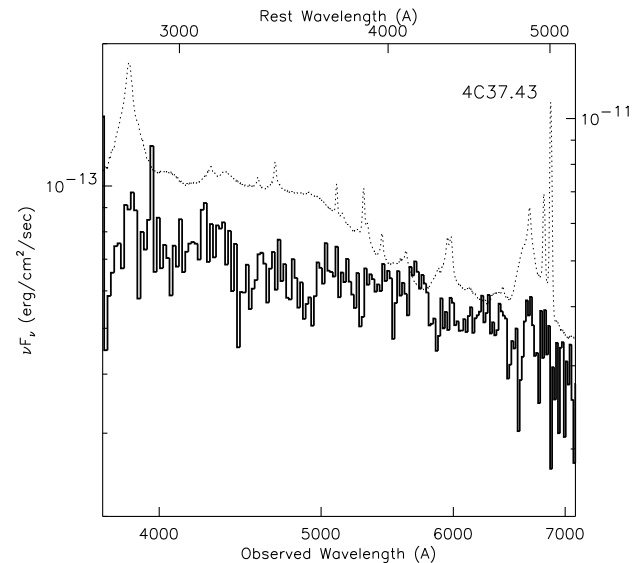


**Figure 8.**  $\nu F_\nu$  plot in log scale for 4C37.43.

2000). Similar probable variations of the polarization have been reported for broad line radio galaxies (e.g. Antonucci 1984). The polarization of the continuum and broad lines in Seyfert 1 galaxies, discussed in section 4.1, are seen to vary on similar time scales (e.g. Young et al. 1999, Smith et al. 2002). We plan to follow up our objects in an upcoming observing run.

#### 4.4 Behavior in the shorter wavelength region

Figures 7 and 8 shows the same data as in Figure 2 and 4 but in  $\nu F_\nu$  instead of  $F_\lambda$ , with the axes on log scales. For Ton 202,  $\nu F_\nu$  has a peak in the wavelength around the Balmer edge feature at least locally. If the total flux has the same spectral shape as the polarized flux, as in the case of polarization being produced in the surrounding electron

scattering region or in the case of a wavelength-independent polarization of the BBB emitter, this implies that the energy output from the small blue bump is much larger than previously thought. Also, in order for the UV continuum to ionize the surrounding region, the BBB emission should turn up as it goes into the shorter wavelength region under the small blue bump. The possible turn-up observed is still uncertain and will be followed up with a new blue sensitive CCD at the Keck. Targets with higher redshifts would be better for the investigation at shorter wavelengths and we have implemented observations at the VLT which will be published elsewhere. We also plan to observe more targets.

#### 4.5 Broadening and Accretion Disk Models

As we have pointed out, even though the high order Balmer absorption lines, and possibly metal lines, are expected to blur the edge substantially, the observed edge feature suggests a broadening probably by a high velocity dispersion of the gas around the nucleus. In this case, very crudely, the velocity dispersion needed is  $\Delta\lambda/\lambda \sim 400/3600 \sim 0.1c$ , corresponding to  $\sim 100R_g$  ( $R_g = GM/c^2$  for a black hole mass  $M$ ) for a Keplerian rotation.

In terms of accretion disc models for quasars, this radius is broadly conceivable for a Balmer edge emitting radius. The preliminary calculation using the model of Hubeny et al. (2000), without any absorption lines show that the observed feature can at least crudely be explained by the emission from the disc atmosphere with the Doppler smearing, although the high order Balmer absorption lines can be crucial to the spectral shape at the edge region. The appropriate model is under development. We stress, however, that our conclusion of an optically-thick thermal BBB emitter does not involve any particular model of the nucleus.

## 5 CONCLUSIONS

We have taken high S/N polarized flux spectra of two quasars with LRISp on the Keck telescope in order to investigate the behavior around the Balmer edge. One of them, Ton 202, shows a slope change at around  $4000\text{\AA}$ . There might also be a possible up-turn at  $3600\text{\AA}$  in the same polarized flux spectrum. We identify this to be a Balmer edge feature, seen in absorption in the shorter wavelength side. There are essentially no broad emission lines in the polarized flux spectrum of Ton 202. This indicates that the polarized flux arises interior to the BLR, showing the spectrum with all the contaminating emissions from the BLR and outer regions scraped off and removed. Therefore, the polarized flux spectrum shape is likely to be intrinsic to the Big Blue Bump emission. In this case, the identified Balmer edge feature indicates that the Big Blue Bump emission is thermal and optically thick.

The polarized flux shape would be intrinsic to the BBB emission in two general cases: (1) the Balmer-edge absorption, its broadening, and polarization are occurring within the BBB emitter itself or (2) the broadened Balmer-edge absorption feature is formed within the BBB emitter, and some part of the emission is subsequently scattered (thus getting polarized) by electrons in an optically-thin region surrounding the BBB emitter. This region would be oblate

in shape and perpendicular to the jet axis in order to produce polarization parallel to the axis.

In another quasar, 4C37.43, there might be a very weak broad component of H $\beta$  line in the polarized flux. This could imply that the polarization arises from scales not much smaller than the BLR. This might be the case in general, so that the case (2) above may be preferred and the size of the postulated oblate scattering region might generally be comparable to the innermost radius of the BLR.

However, we cannot rule out some cases where the Balmer-edge feature is not intrinsic to the BBB emission. The Balmer-edge absorption feature might be formed within the scattering region surrounding the featureless BBB emitter, along with the polarization. However in this case, the scattering/absorbing region should be rather optically thick and in a rather deep potential well, which might make this case almost equivalent to the case (1) above. It might also be possible to postulate (possibly independent) compact featureless polarized flux emitter and have the absorption and broadening in a foreground region, but this would require a particular velocity structure, and the absorption at the Lyman edge would be implausibly large.

## ACKNOWLEDGMENTS

The authors thank A. Barth, D. Leonard, A. Cimatti for helping us to clarify the polarization measurements on the null standard star, E. Agol for providing calibration data, and R. Goodrich for various information on the Keck polarimetry.

## REFERENCES

- Agol, E., Blaes, O., 1996, MNRAS, 282, 965
- Agol, E., Blaes, O., Ionescu-Zanetti, C. 1998, MNRAS, 293, 1
- Antonucci, R. 1983, Nature, 303, 158
- Antonucci, R. 1984, ApJ, 278, 499
- Antonucci, R. 1988, in Supermassive Black Holes, ed. M. Kafatos (Cambridge: Cambridge Univ. Press), 26
- Antonucci, R. 1999, in High Energy Processes in Accreting Black Holes, ASP Conf. Ser. 161, 193
- Antonucci, R. 2002, in Astrophysical Spectropolarimetry (Cambridge: Cambridge Univ. Press) 151
- Antonucci, R., Kinney, A. L., Ford, H. C. 1989, ApJ, 342, 64
- Blaes, O., Hubeny, I., Agol, E., Krolik, J. H. 2001, ApJ, 563, 560
- Berriman, G., Schmidt, G. D., West, S. C., Stockman, H. S., 1990, ApJS, 74, 869
- Brown, J. C., McLean, I. S., 1977, A&A, 57, 141
- Chandrasekar, S. 1960, Radiative Transfer (New York: Dover)
- Coleman, H. H., Shields, G. A., 1990, ApJ, 363, 415
- Czerny, B., Zbyszewska, M., 1991, MNRAS, 249, 634
- Francis, P. J., Hewett, P. C., Foltz, C. B., Chaffee, F. H., Weymann, R. J., Morris, S. L. 1991, ApJ, 373, 465
- Goodrich, R. W., Miller, J. S. 1994, ApJ, 434, 82
- Gnedin, Yu. N., Silant'ev, N. A., 1978, SvA, 22, 325

- Hubeny, I., Agol, E., Blaes, O., Krolik, J. H., 2000, *ApJ*, 533, 710
- Hubeny, I., Blaes, O., Krolik, J. H., Agol, E., 2001, *ApJ*, 559, 680
- Neugebauer, G., Green, R. F., Matthews, K., Schmidt, M., Soifer, B. T., Bennett, J. 1987, *ApJS*, 63, 615
- Koratkar, A., Blaes, O., 1999, *PASP*, 111, 1
- Koratkar, A., Kinney, A. L., Bohlin, R. C. 1992, *ApJ*, 400, 435
- Kriss, G. A., Davidsen, A. F., Zheng, W., Lee, G., 1999, *ApJ*, 527, 683
- Lanzetta, K. M., Turnshek, D. A., Sandoval, J., 1993, *ApJS*, 84, 109
- Laor, A., Netzer, H., Piran, T., 1990, *MNRAS*, 242, 560
- Miller, J. S., Robinson, L. B., Goodrich, R. W., 1988, in *Instrumentation for Ground-Based Astronomy*, ed. L. B. Robinson (New York, Springer), p. 157
- Sanders, D. B., Phinney, E. S., Neugebauer, G., Soifer, B. T., Matthews, K., 1989, *ApJ*, 347, 29
- Schmidt, G. Elston, R., Lupie, O. L., 1992, *AJ*, 104, 1563
- Schmidt, G., Smith, P., 2000, *ApJ*, 545, 117
- Smith, J. E., Young, S., Robinson, A., Corbett, E. A., Giannuzzo, M. E., Axon, D. J., Hough, J. H. 2002, *MNRAS*, 335, 773
- Young, S., Corbett, E. A., Giannuzzo, M. E., Hough, J. H., Robinson, A., Bailey, J. A., Axon, D. J. 1999, *MNRAS*, 303, 227
- Zheng, W., Kriss, G. A., Telfer, R. C., Grimes, J. P., Davidsen, A. F., 1997, *ApJ*, 475, 469